Tokyo Climate Center, Japan Meteorological Agency

TCC News

Spring 2026

Table of Contents: TCC News No. 84

JMA's Seasonal Numerical Ensemble Prediction for Boreal Summer 2026

This report outlines JMA's dynamical seasonal ensemble prediction for boreal summer 2026 (June – August, referred to as JJA), which was used as a basis for JMA's operational three-month outlook issued on 19 May 2026. The outlook is based on the seasonal ensemble prediction system with the coupled atmosphere-ocean general circulation model (CGCM).

Summary: Based on JMA's seasonal ensemble prediction system, it is likely (90%) that El Niño conditions will develop by boreal summer. With NINO.3 sea surface temperatures (SSTs) expected to reach above-normal levels by boreal summer, convective activity is predicted to be enhanced over the central tropical Pacific and suppressed from the Indian Ocean to Indonesia. In the lower troposphere, cyclonic circulation anomalies straddling the equator are predicted around the Maritime Continent. The monsoon trough is predicted to be deeper than normal over the sea east of the Philippines.

1. Sea surface temperatures

Figure 1-1 shows predicted SSTs (contours) and related anomalies (shading) for JJA. JMA's seasonal ensemble prediction system forecasts that NINO.3 SSTs will rise to above normal by boreal summer in association with further increased presence of warm subsurface water and its eastward propagation in the equatorial Pacific. In conclusion, it is likely (90%) that El Niño conditions will develop by boreal summer. In the western tropical Pacific, SSTs are expected to decrease by the end of boreal summer, and are likely to reach below normal by boreal autumn. In the tropical Indian Ocean, SSTs are likely to be near normal until autumn.

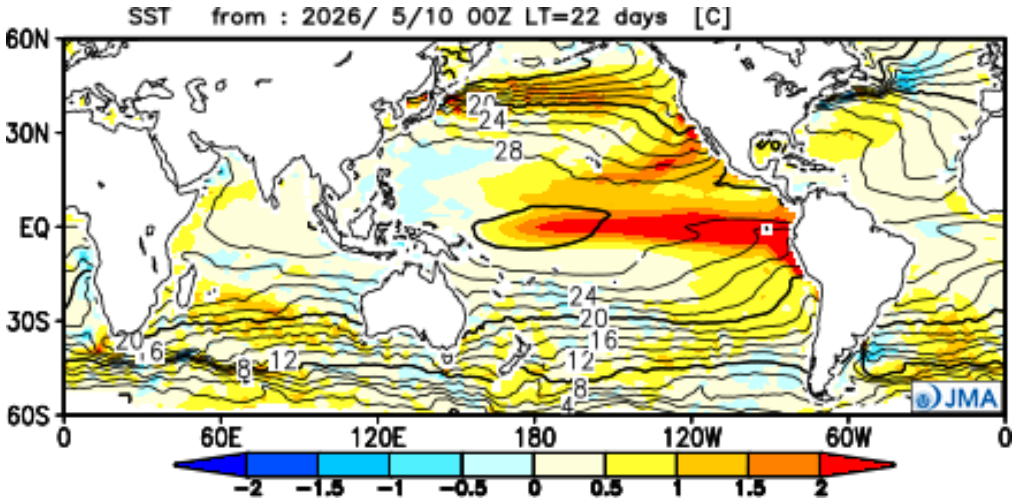

Figure 1-1 Predicted SSTs (contours) and SST anomalies (shading) for June–August 2026 (ensemble mean of 85 members)

2. Prediction for the tropics and sub-tropics

Figure 1-2 (a) shows predicted velocity potential (contours) and its anomalies (shading) in the upper troposphere for JJA. Large-scale divergence anomalies are predicted over the central part of the tropical Pacific, while large-scale convergence anomalies are predicted over the Indian Ocean.

Figure 1-2 (b) shows predicted stream functions (contours) and its anomalies (shading) in the upper troposphere for JJA. Cyclonic and anti-cyclonic circulation anomalies are predicted from Africa to the Indian Ocean and over the tropical western Pacific, respectively, in association with tropical convective activity.

Figure 1-2 (c) shows predicted stream functions (contours), its anomalies (shading), and wind vector anomalies (vector) in the lower troposphere for JJA. Cyclonic circulation anomalies straddling the equator are predicted around the Maritime Continent.

Figure 1-2 (d) shows predicted sea level pressure (contours) and its anomalies (shading) for JJA. Positive anomalies are predicted over the Indian Ocean. The monsoon trough is predicted to be deeper than normal over the sea east of the Philippines.

(a)

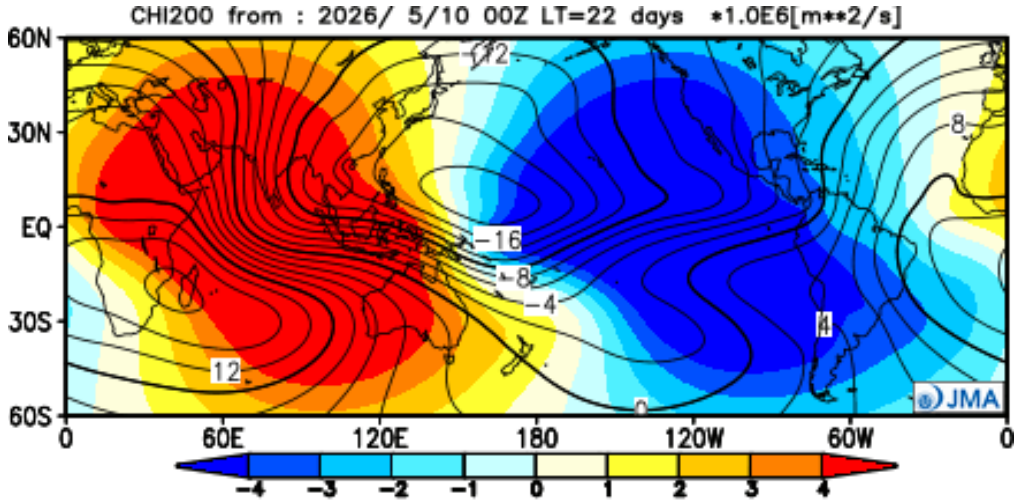

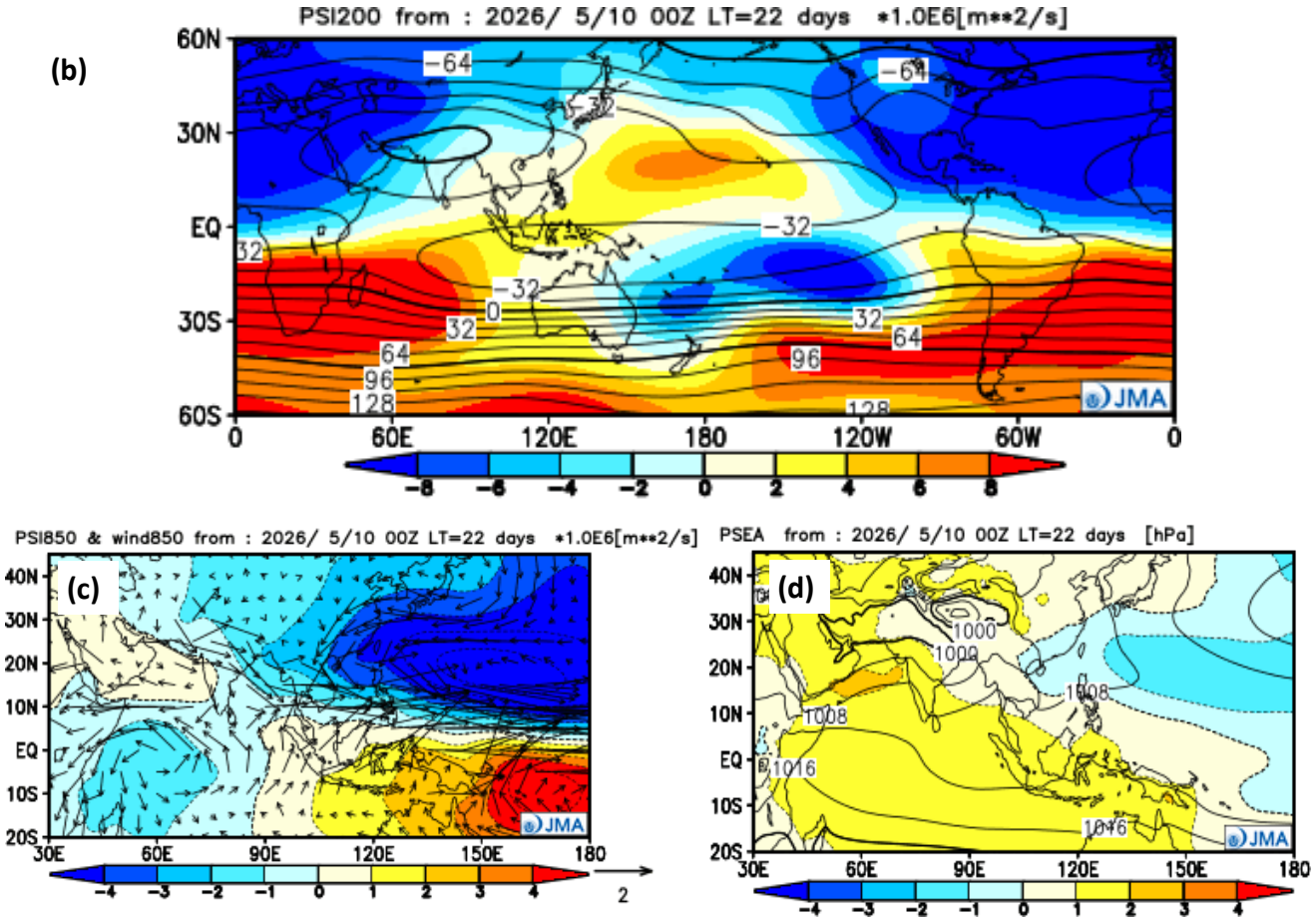

Figure 1-2 Predicted atmospheric fields for June–August 2026 (ensemble mean of 85 members)

(a) Velocity potential over 60°N-60°S at 200-hPa (contours) and anomaly (shading). The contour interval is 2×10^6 m^2/s.

(b) Stream function over 60°N-60°S at 200-hPa (contours) and anomaly (shading). The contour interval is 16×10^6 m^2/s.

(c) Stream function over Asian region at 850-hPa (contours), its anomaly (shading) and wind vector anomaly (vector). The contour interval is 5×10^6 m^2/s.

(d) Sea level pressure over Asian region (contours) and anomaly (shading). The contour interval is 4 hPa.

3. Prediction for the mid- and high- latitudes of the Northern Hemisphere

Figure 1-3 (a) shows predicted 500-hPa geopotential heights (contours) and related anomalies (shading) for JJA. Positive anomalies are predicted over a wide area of the Northern Hemisphere.

Figure 1-3 (b) shows predicted sea level pressure (contours) and related anomalies (shading) for JJA. The North Pacific subtropical high is predicted to be weaker than normal, especially in the southwestern part.

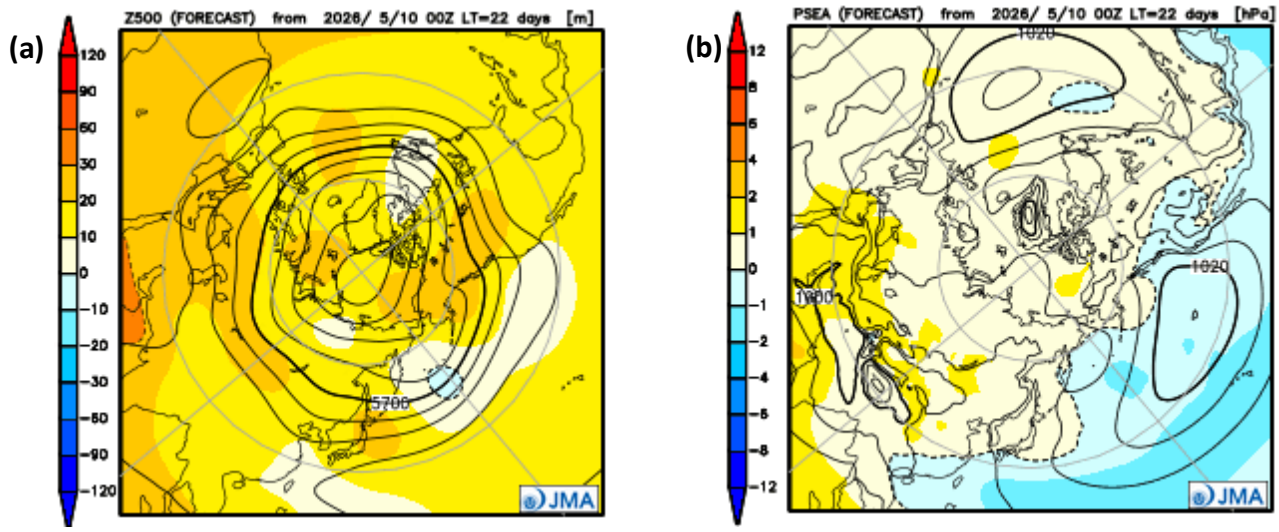

Figure 1-3 Predicted atmospheric fields over 20°N-90°N for June–August 2026 (ensemble mean of 85 members)
(a) Geopotential height at 500-hPa (contours) and anomaly (shading). The contour interval is 60 m.
(b) Sea level pressure (contours) and anomaly (shading). The contour interval is 4 hPa.

Note: JMA operates a seasonal Ensemble Prediction System (EPS) using its Coupled atmosphere-ocean General Circulation Model (CGCM) to issue one-month predictions, three-month predictions, warm/cold season outlooks and El Niño Outlooks. The EPS produces perturbed initial conditions by means of a combination of the initial perturbation method and the lagged average forecasting (LAF) method. Prediction is made using 85 members from the latest 17 initial dates (5 members are used every day). Details of the prediction system and verification maps based on 30-year hindcast experiments (1991–2020) are available at https://ds.data.jma.go.jp/wmc/products/model/.

(KYODA Masayuki, Tokyo Climate Center)

<<Table of contents <Top of this article

Summary of the 2025/2026 Asian Winter Monsoon

This report summarizes the characteristics of the surface climate and atmospheric/oceanographic conditions related to the Asian winter monsoon for 2025/2026.

Note: Dataset of the Japanese Reanalysis for Three Quarters of a century (JRA-3Q) (Kosaka et al. 2024) and MGDSST (Kurihara et al. 2006) were used to analyze atmospheric circulation and sea surface temperature (SST). NOAA Climate Prediction Center (CPC) Blended Outgoing Longwave Radiation (OLR) data provided by the U.S. NOAA Physical Sciences Laboratory (PSL) from their web site at https://psl.noaa.gov/data/gridded/data.cpc_blended_olr-2.5deg.html was used to infer tropical convective activity. The base period for the normal is 1991 to 2020. The term "anomaly" as used in this report refers to deviation from the normal.

1. Surface climate conditions

In winter 2025/2026, three-month (DJF) mean temperatures were above normal over Eastern Siberia and wide areas from South Asia to East Asia, and below normal from Western Siberia to Central Siberia (Figure 2-1 (a)). Above-

normal temperatures were observed from South Asia to around China, particularly in December and February (Figures 2-1 (b) and (d)), indicating weaker-than-normal accumulation of cold-air masses over the area. Below-normal temperatures were particularly observed from Western and Central Siberia to Japan in January (Figure 2-1 (c)), indicating temporarily enhanced cold-air outflows toward East Asia. Winter precipitation amounts were generally above normal over Eastern Siberia and from southern Central Siberia to Central Asia, and were mostly below normal in and around China (Figure 2-2).

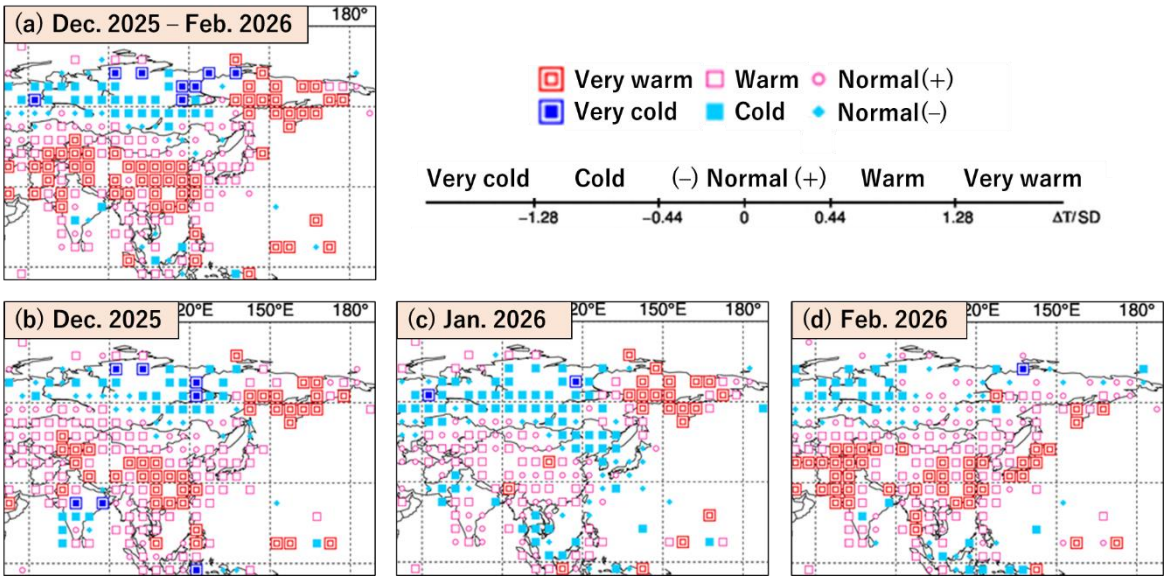

Figure 2-1 Temperature anomalies for (a) December 2025 to February 2026, (b) December 2025, (c) January 2026 and (d) February 2026

Categories are defined by the three-month/monthly mean temperature anomaly against the normal divided by its standard deviation and averaged in 5° × 5° grid boxes. The thresholds of each category are –1.28, –0.44, 0, +0.44 and +1.28. Standard deviations were calculated from 1991 – 2020 statistics. Areas over land without graphical marks are those where observation data are insufficient or where normal data are unavailable.

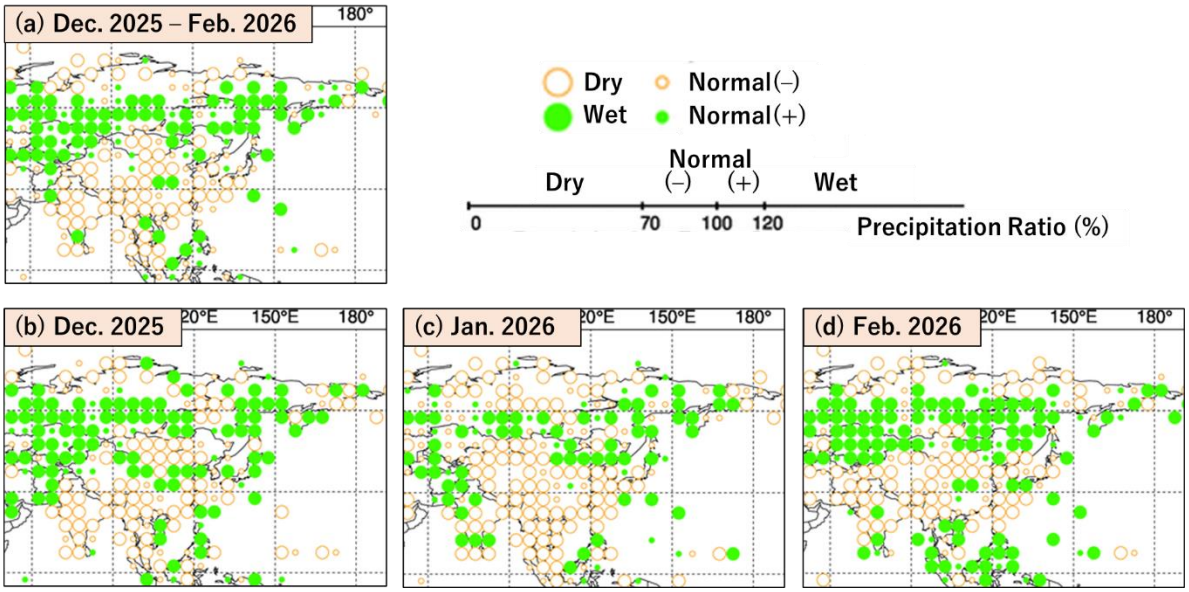

Figure 2-2 Precipitation ratio for (a) December 2025 to February 2026, (b) December 2025, (c) January 2026 and (d) February 2026

Categories are defined by the three-month/monthly precipitation ratio against the normal and averaged in 5° × 5° grid boxes. The thresholds of each category are 70, 100 and 120%. Areas over land without graphical marks are those where observation data are insufficient or where normal data are unavailable.

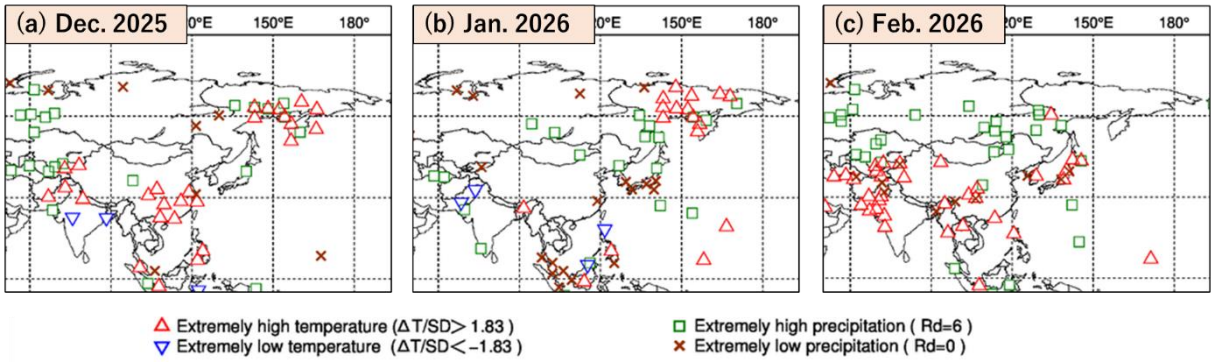

Figure 2-3 Extreme climate stations for (a) December 2025, (b) January 2026 and (c) February 2026

ΔT, SD and Rd indicate temperature anomaly, standard deviation and quintile, respectively.

Figure 2-3 plots stations where extreme climatic conditions were observed from December 2025 to February 2026. Extremely high temperatures were observed in Eastern Siberia from December to January (Figures 2-3 (a) and (b)) and in Pakistan and South China in December and February (Figures 2-3 (a) and (c)). Extremely high precipitation amounts were observed from Western Siberia to Central Asia in December and in southern Siberia in February (Figures 2-3 (a) and (c)). Extremely low precipitation amounts were seen in and around western Japan in January (Figure 2-3 (b)).

2. Characteristic atmospheric circulation and oceanographic conditions

This section presents characteristics of atmospheric circulation and oceanographic conditions averaged in winter 2025/2026.

2.1 Conditions in the tropics

Figure 2-4 shows three-month mean anomalies of sea surface temperature (SST), convective activity, and the upper-tropospheric large-scale divergence in winter 2025/2026. Notably positive SST anomalies were dominant in western parts of the equatorial Pacific, while negative values were observed in central and eastern parts (Figure 2-4 (a)). This anomaly pattern resembled typical La Niña conditions, although it did not meet JMA's official criteria for the declaration of a La Niña event. Significantly positive SST anomalies were observed in the mid-latitudes of the North Pacific and in the subtropical North Atlantic, while values in the Indian Ocean were near-normal to positive. Convective activity inferred from OLR was enhanced from the Maritime Continent to the western Pacific and over equatorial Africa, and suppressed over the Indian Ocean and from the central-to-eastern Pacific. Convective activity was also significantly enhanced in the subtropical-western to central North Pacific (Figure 2-4 (b)). In the upper troposphere, large-scale divergence anomalies were dominant from the Maritime Continent to the subtropical central North Pacific and over equatorial Africa (Figure 2-4 (b)). Large-scale convergence anomalies were seen over the Indian Ocean and from the central-to-eastern Pacific (Figure 2-4 (b)).

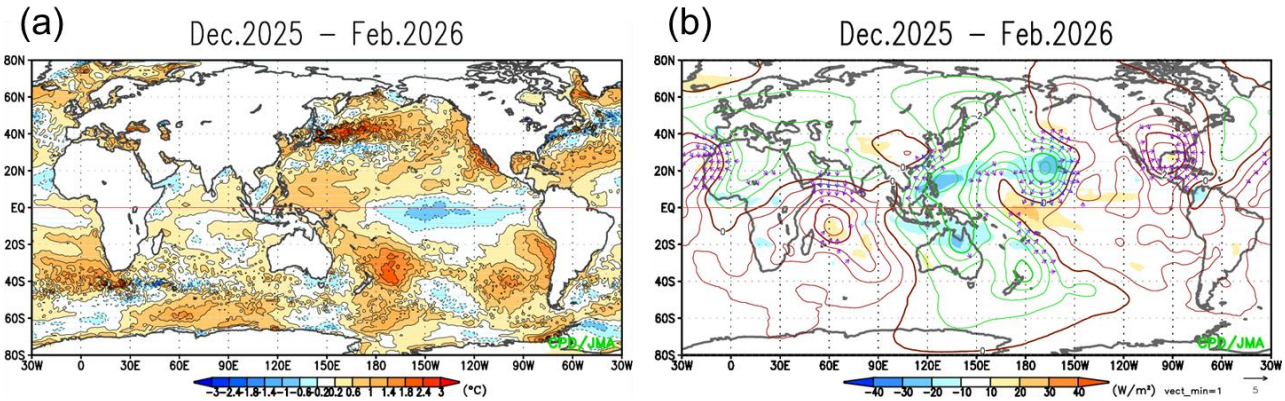

Figure 2-4 Three-month mean (a) SST anomalies and (b) anomalous convective activity in winter 2025/2026

The shadings in (a) and (b) show the SST anomalies [°C] and OLR anomalies [W/m^2]. The contours and vectors in (b) indicate 200-hPa velocity potential anomalies at intervals of 0.5 × 10^6 m^2/s and divergent wind anomalies, respectively. Negative (cold color) and positive (warm color) OLR anomalies show enhanced and suppressed convective activity compared to the normal, respectively.

Figure 2-5 shows three-month mean 200- and 850-hPa stream function anomalies for winter 2025/2026. In the upper troposphere, a pair of weak anti-cyclonic circulation anomalies straddled the equator from the eastern Indian Ocean to the western Pacific, and a pair of cyclonic circulation anomalies straddled the equator from the central to eastern Pacific. Cyclonic circulation anomalies over the central Pacific extended northward to around 40°N (Figure 2-5 (a)). In the tropical lower troposphere, pairs of cyclonic and anticyclonic circulation anomalies straddled the equator over the central Pacific and from the eastern Indian Ocean to the western Pacific (Figure 2-5 (b)).

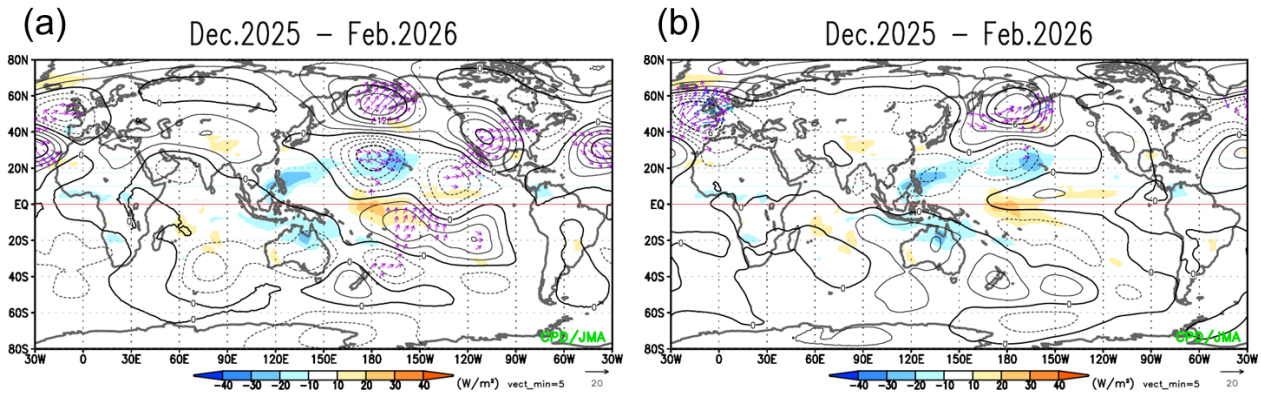

Figure 2-5 Three-month mean (a) 200-hPa and (b) 850-hPa stream function anomalies in winter 2025/2026

The contours indicate stream function anomalies at intervals of (a) 5 × 10^6 m^2/s and (b) 2.5 × 10^6 m^2/s, and the shadings show OLR anomalies [W/m^2]. The vectors denote horizontal component of wave activity flux [m^2/s^2] defined by Takaya and Nakamura (2001).

2.2 Conditions in the Northern Hemisphere extratropics

Figure 2-6 shows three-month mean 500-hPa height, sea level pressure (SLP), and 850-hPa temperature in winter 2025/2026 in the Northern Hemisphere. In the 500-hPa height field (Figure 2-6 (a)), the polar vortex exhibited a split, with the main vortex located over northern Canada. Significantly positive height anomalies were seen around Greenland and the Bering Sea, where blocking highs were frequently observed. Negative anomalies were also observed from western Siberia to Primorsky Krai, corresponding to the southward meandering of the polar front jet stream (PFJ) over Eurasia. In the SLP field, the Siberian High and the Aleutian Low were both weaker than normal,

indicating a weaker-than-normal East Asian winter monsoon (Figure 2-6 (b)). Temperatures at 850 hPa were above normal over a wide mid-latitude area and below normal from Western Siberia to Central Siberia (Figure 2-6 (c)), in line with the 500-hPa height and SLP anomalies described above.

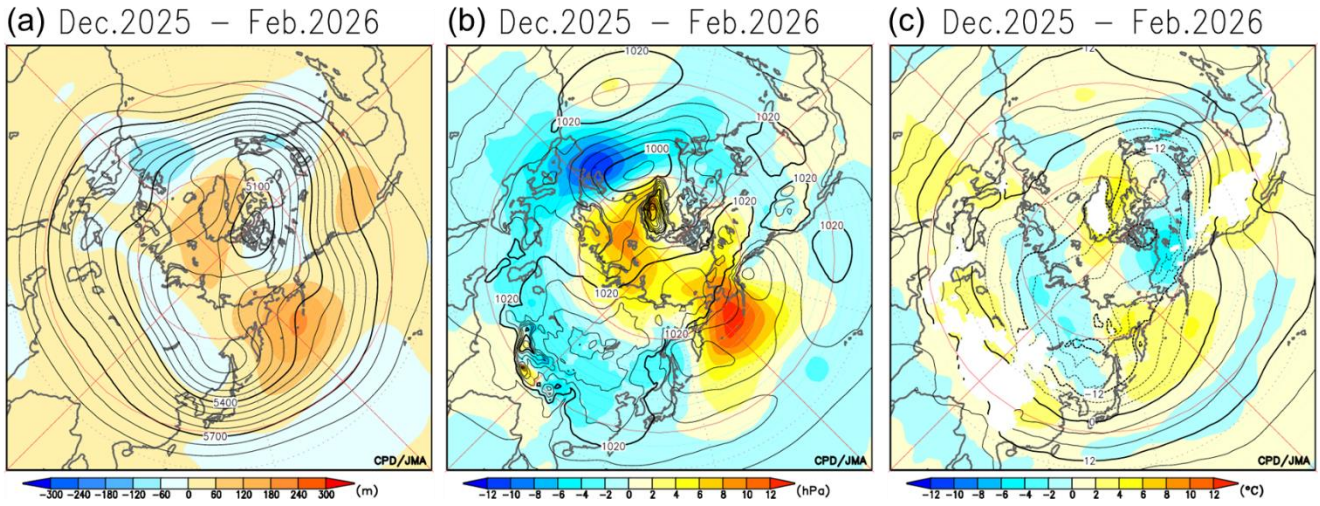

Figure 2-6 Three-month mean (a) 500-hPa height, (b) sea level pressure, and (c) 850-hPa temperature in winter 2025/2026
The contour intervals are (a) 60 m, (b) 4 hPa, and (c) 4 °C. The shading denotes related anomalies.

2.3 Cold spells in East Asia

As another notable winter characteristic, several cold spells hit East Asia in the second half of January to early February in association with intensified blocking highs over Alaska and Greenland (Figures 2-7 (a) and (b)) along with the processes of vertical coupling (e.g., Ambaum and Hoskins 2002, Perlwitz and Harnik 2004, Mukougawa and Hirooka 2007) and downward Rossby wave packet propagation (e.g., Kodera et al. 2008, Kodera et al. 2013) (Figure 2-7 (c)), leading to the development and persistence of a negative Arctic Oscillation (AO). The westerly jet stream also shifted southward from its normal position around East Asia (Figure 2-7 (d)), bringing strong cold-air flows over East Asia (Figure 2-7 (e)). In Japan, heavy snowfall continued for two weeks in northern Tohoku, and Aomori City recorded its highest maximum snow depth in 40 years. In the first half of February, the split tropospheric polar vortex shifted southward toward the Sea of Okhotsk. The negative AO phase persisted into early February, favoring southward intrusions of cold air into East Asia (not shown). Cold vortices frequently moved from central Siberia toward East Asia, resulting in repeated southward intrusions of upper-level cold air. The development and persistence of a negative AO was potentially a primary factor behind the periodic cold spells observed in East Asia in the second half of January to early February 2026.

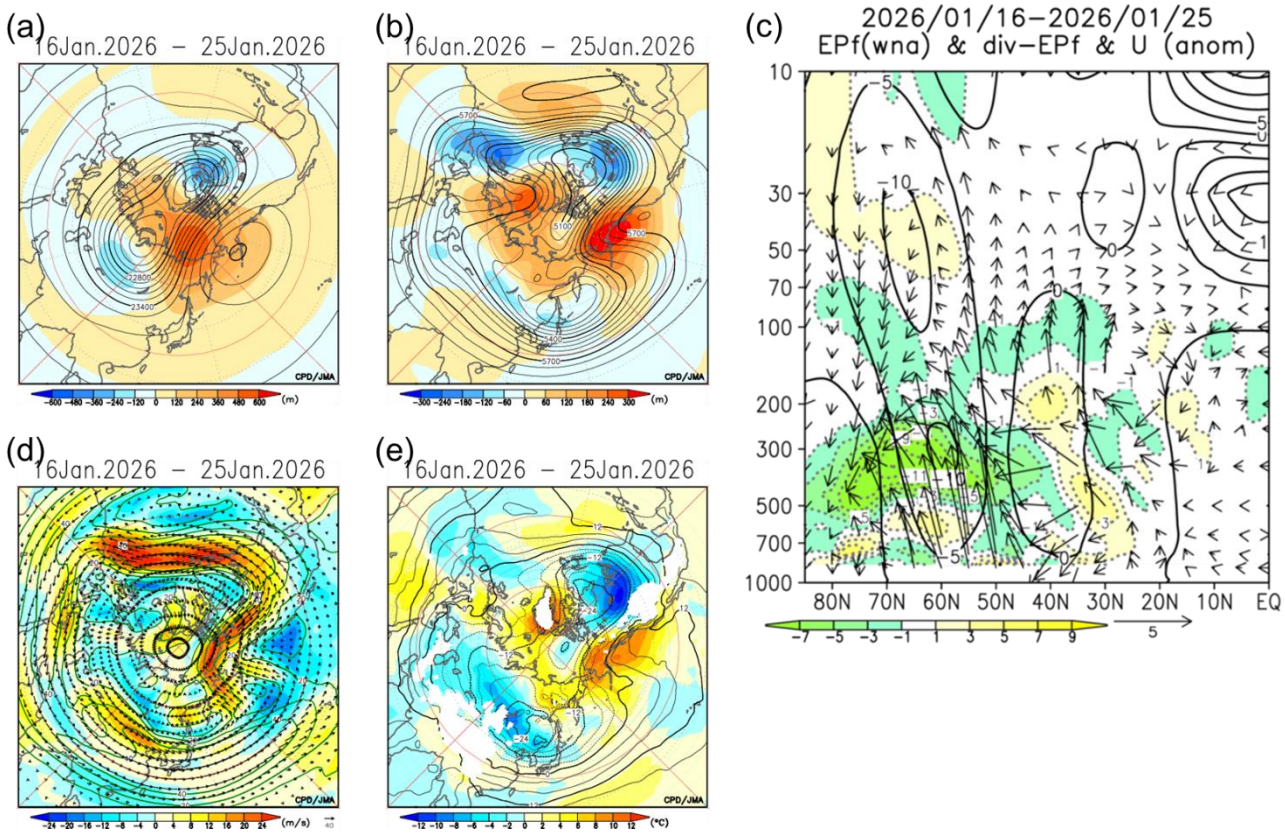

Figure 2-7 (a) 30-hPa height, (b) 500-hPa height, (c) Latitude–height cross section of zonal-mean zonal wind anomalies and Eliassen–Palm (E-P) flux anomalies, (d) 300-hPa wind speed and wind vector, (e) 850-hPa temperature, averaged from 16th to 25th January 2026.

The contour intervals are (a) 120 m, (b) 60 m, (c) 5 m/s, (d) 10 m/s, and (e) 4°C. Shading (a, b, d, e) shows related anomalies and (c) divergence of E-P flux, and vectors in (c) indicate vertical components of E-P flux.

References

Ambaum, M. H., and B. J. Hoskins, 2002: The NAO troposphere–stratosphere connection. *J. Climate*, **15**, 1969–1978, doi:10.1175/1520-0442(2002)015<1969:TNTSC>2.0.CO;2.

Kurihara, Y., T. Sakurai, and T. Kuragano, 2006: Global daily sea surface temperature analysis using data from satellite microwave radiometer, satellite infrared radiometer and in-situ observations. *Weather Service Bulletin*, **73**, Special issue, s1-s18 (in Japanese).

Kodera, K., H. Mukougawa, and S. Itoh, 2008: Tropospheric impact of reflected planetary waves from the stratosphere. *Geophys. Res. Lett.*, **35**, L16806, doi:10.1029/2008GL034575.

Kodera, K., H. Mukougawa, and A. Fujii, 2013: Influence of the vertical and zonal propagation of stratospheric planetary waves on tropospheric blockings. *J. Geophys. Res. Atmos.*, **118**, doi:10.1002/jgrd.50650.

Kosaka, Y., S. Kobayashi, Y. Harada, C. Kobayashi, H. Naoe, K. Yoshimoto, M. Harada, N. Goto, J. Chiba, K. Miyaoka, R. Sekiguchi, M. Deushi, H. Kamahori, T. Nakaegawa; T. Y. Tanaka, T. Tokuhiro, Y. Sato, Y. Matsushita, and K. Onogi, 2024: The JRA-3Q reanalysis. *J. Meteor. Soc. Japan*, **102**, 49-109. https://doi.org/10.2151/jmsj.2024-004.

Mukougawa, H., and T. Hirooka, 2007: Predictability of the downward migration of the Northern Annular Mode: A

case study for January 2003. *J. Meteor. Soc. Japan*, **85**, 861-870.

Perlwitz, J., and N. Harnik, 2004: Downward coupling between the stratosphere and troposphere: The relative roles of wave and zonal mean processes. *J. Climate*, **17**, 4902–4909, doi:10.1175/JCLI-3247.1.

(*KAYABA Nobuyuki, YAMADA Ken, Tokyo Climate Center*)

<<Table of contents <Top of this article

TCC and WMC Tokyo co-contributions to Regional Climate Outlook Forums in Asia

WMO Regional Climate Outlook Forums (RCOFs) bring together national, regional and international climate experts on an operational basis to produce regional climate outlooks based on inputs from participating NMHSs, regional institutions, Regional Climate Centres (RCCs) and global producers of climate predictions. By providing a platform for countries with similar climatological characteristics to discuss related matters, these forums ensure consistency in terms of access to and interpretation of climate information. In spring 2026, TCC experts participated in the following two RCOFs in Asia.

- The 34th summer session of the South Asian Climate Outlook Forum (SASCOF-34)
- The 22nd session of the Forum on Regional Climate Monitoring, Assessment and Prediction for Regional Association II (FOCRA II-22)

1. SASCOF-34

RCC Pune hosted the 34th summer session of the South Asian Climate Outlook Forum (SASCOF-34) and Climate Services User Forum (CSUF) from 28 to 30 April 2026 in Male, Maldives. As part of WMO World Meteorological Centre (WMC) and TCC joint activities (co-activities), a JMA expert made two presentations as detailed below. These contributed to discussions on the climate outlook for South Asia, and are expected to support the output of country-scale outlooks by National Meteorological and Hydrological Services (NMHSs) in the relevant regions.

- Summer monsoon season outlook based on JMA's operational seasonal ensemble prediction system (JMA/MRI-CPS4) with probabilistic information on oceanographic conditions from the Indian Ocean to the Pacific (El Niño southern oscillation, Indian Ocean Dipole, etc.) and associated atmospheric circulation patterns
- Recent joint activities involving WMC Tokyo and TCC roles, such as upgrading of the Interactive Tool for Analysis of the Climate System (iTacs6) and special reporting on heavy rainfall in and around Southeast Asia in November 2025

SASCOF-34 issued a climate outlook for the 2026 summer monsoon season (June – September). The subsequent CSUF session focused on dialogue with user sectors, including those of water, agriculture, disaster risk reduction and health. In particular, discussions addressed ways to interpret seasonal forecast uncertainty and highlighted South Asia's Heat and Health Initiative.

Presentation at the SASCOF

Discussions at the SASCOF

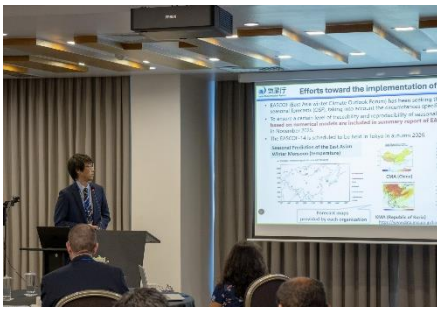

Presentation at the CSUF

Group photo at the conference center

(Photos provided by SASCOF)

2. FOCRA II-22

The 22nd Session of the Forum on Regional Climate Monitoring, Assessment and Prediction for Asia (FOCRA II-22) was held from 13 to 15 May 2026 in Nanjing, China. This meeting was attended by 168 representatives from the WMO Secretariat and over 20 countries and regions, including Asia, Russia, the United Kingdom, the Pacific Islands and Africa. Attendees shared recent research results and discussed climate service development, new technologies and applications such as AI, and climate projection and seasonal climate prediction.

JMA representatives gave two presentations on the following:

- Characteristics of record-high temperatures in Japan during the past three summers, based on analysis of differences in mean fields between these and earlier summers.
- Seasonal outlook for summer over Japan, including probabilistic forecasts, based on oceanographic conditions from the Indian Ocean to the Pacific and associated atmospheric circulation patterns predicted by JMA/MRI-CPS4

FOCRA II-22 issued a consensus outlook for summer climate conditions in the RA II region after discussions in the summary session. Broad agreement was reached on enhancing collaboration between RCCs and NMHSs toward the production of enhanced climate information for RA II.

Presentation at FOCRA II

Presentation at FOCRA II

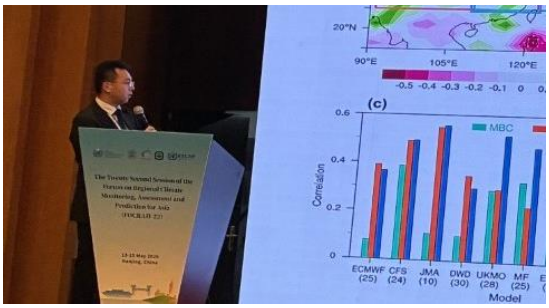

Presentation at FOCRA II

Group photo (provided by FOCRA II)

(SASCOF-34: YAMADA Ken, FOCRA II-22: KYOUDA Masayuki and MITSUKAWA Yuhei, Tokyo Climate Center)

<<Table of contents <Top of this article

You can find the latest newsletter from the Japan International Cooperation Agency (JICA).

JICA Magazine

https://jicamagazine.jica.go.jp/en/

"JICA magazine" is a public relations magazine published by JICA. It introduces the current situations of developing countries around the world, the people who are active in the field, and the content of their activities.

Any comments or inquiries about this newsletter and/or the TCC website would be much appreciated.
Please send e-mail to tcc@met.kishou.go.jp.
(Editors: NODA Rikuo)

Tokyo Climate Center, Japan Meteorological Agency
3-6-9 Toranomon, Minato City, Tokyo 105-8431, Japan

TCC Website:
https://www.data.jma.go.jp/tcc/tcc/index.html